# 24. DARK MATTER

Revised September 2013 by M. Drees (Bonn University) and G. Gerbier (Saclay, CEA).

## 24.1. Theory

### 24.1.1. *Evidence for Dark Matter* :

The existence of Dark (*i.e.*, non-luminous and non-absorbing) Matter (DM) is by now well established [1,2]. The earliest, and perhaps still most convincing, evidence for DM came from the observation that various luminous objects (stars, gas clouds, globular clusters, or entire galaxies) move faster than one would expect if they only felt the gravitational attraction of other visible objects. An important example is the measurement of galactic rotation curves. The rotational velocity $v$ of an object on a stable Keplerian orbit with radius $r$ around a galaxy scales like $v(r) \propto \sqrt{M(r)/r}$, where $M(r)$ is the mass inside the orbit. If $r$ lies outside the visible part of the galaxy and mass tracks light, one would expect $v(r) \propto 1/\sqrt{r}$. Instead, in most galaxies one finds that $v$ becomes approximately constant out to the largest values of $r$ where the rotation curve can be measured; in our own galaxy, $v \simeq 240$ km/s at the location of our solar system, with little change out to the largest observable radius. This implies the existence of a *dark halo*, with mass density $\rho(r) \propto 1/r^2$, *i.e.*, $M(r) \propto r$; at some point $\rho$ will have to fall off faster (in order to keep the total mass of the galaxy finite), but we do not know at what radius this will happen. This leads to a lower bound on the DM mass density, $\Omega_{\rm DM} \gtrsim 0.1$, where $\Omega_X \equiv \rho_X/\rho_{\rm crit}$, $\rho_{\rm crit}$ being the critical mass density (*i.e.*, $\Omega_{\rm tot} = 1$ corresponds to a flat Universe).

The observation of clusters of galaxies tends to give somewhat larger values, $\Omega_{\rm DM} \simeq 0.2$. These observations include measurements of the peculiar velocities of galaxies in the cluster, which are a measure of their potential energy if the cluster is virialized; measurements of the *X-ray* temperature of hot gas in the cluster, which again correlates with the gravitational potential felt by the gas; and—most directly—studies of (weak) gravitational lensing of background galaxies on the cluster.

A particularly compelling example involves the bullet cluster (1E0657-558) which recently (on cosmological time scales) passed through another cluster. As a result, the hot gas forming most of the clusters' baryonic mass was shocked and decelerated, whereas the galaxies in the clusters proceeded on ballistic trajectories. Gravitational lensing shows that most of the total mass also moved ballistically, indicating that DM self-interactions are indeed weak [1].

The currently most accurate, if somewhat indirect, determination of $\Omega_{\rm DM}$ comes from global fits of cosmological parameters to a variety of observations; see the Section on Cosmological Parameters for details. For example, using measurements of the anisotropy of the cosmic microwave background (CMB) and of the spatial distribution of galaxies, Ref. 3 finds a density of cold, non-baryonic matter

$$\Omega_{\rm nbm} h^2 = 0.1198 \pm 0.0026 \ , \tag{24.1}$$

where $h$ is the Hubble constant in units of 100 km/(s·Mpc). Some part of the baryonic matter density [3],

$$\Omega_{\rm b} h^2 = 0.02207 \pm 0.00027 \ , \tag{24.2}$$

may well contribute to (baryonic) DM, *e.g.*, MACHOs [4] or cold molecular gas clouds [5].

The DM density in the "neighborhood" of our solar system is also of considerable interest. This was first estimated as early as 1922 by J.H. Jeans, who analyzed the motion of nearby stars transverse to the galactic plane [2]. He concluded that in our galactic neighborhood, the average density of DM must be roughly equal to that of luminous matter (stars, gas, dust). Remarkably enough, the most recent estimate finds a quite similar result for the smooth component of the local Dark Matter density [6]:

$$\rho_{\rm DM}^{\rm local} = (0.39 \pm 0.03) \frac{\rm GeV}{\rm cm^3} \ . \tag{24.3}$$

This value may have to be increased by a factor of $1.2 \pm 0.2$ since the baryons in the galactic disk, in which the solar system is located, also increase the local DM density [7]. Small substructures (minihaloes, streams) are not likely to change the local DM density significantly [1]. Note that Eq. (24.3) has been derived by fitting a complete model of our galaxy to a host of data, including the galactic rotation curve. A "purely local" analysis, only using the motion of nearby stars, gives a consistent result, with an error three times as large [8].

### 24.1.2. *Candidates for Dark Matter* :

Analyses of structure formation in the Universe indicate that most DM should be "cold" or "cool", *i.e.*, should have been non-relativistic at the onset of galaxy formation (when there was a galactic mass inside the causal horizon) [1]. This agrees well with the upper bound [3] on the contribution of light neutrinos to Eq. (24.1),

$$\Omega_\nu h^2 \leq 0.0062 \quad 95\% \text{ CL} \ . \tag{24.4}$$

Candidates for non-baryonic DM in Eq. (24.1) must satisfy several conditions: they must be stable on cosmological time scales (otherwise they would have decayed by now), they must interact very weakly with electromagnetic radiation (otherwise they wouldn't qualify as *dark* matter), and they must have the right relic density. Candidates include primordial black holes, axions, sterile neutrinos, and weakly interacting massive particles (WIMPs).

Primordial black holes must have formed before the era of Big-Bang nucleosynthesis, since otherwise they would have been counted in Eq. (24.2) rather than Eq. (24.1). Such an early creation of a large number of black holes is possible only in certain somewhat contrived cosmological models [9].

The existence of axions [10] was first postulated to solve the strong *CP* problem of QCD; they also occur naturally in superstring theories. They are pseudo Nambu-Goldstone bosons associated with the (mostly) spontaneous breaking of a new global "Peccei-Quinn" (PQ) U(1) symmetry at scale $f_a$; see the Section on Axions in this *Review* for further details. Although very light, axions would constitute cold DM, since they were produced non-thermally. At temperatures well above the QCD phase transition, the axion is massless, and the axion field can take any value, parameterized by the "misalignment angle" $\theta_i$. At $T \lesssim 1$ GeV, the axion develops a mass $m_a \sim f_\pi m_\pi / f_a$ due to instanton effects. Unless the axion field happens to find itself at the minimum of its

potential ($\theta_i = 0$), it will begin to oscillate once $m_a$ becomes comparable to the Hubble parameter $H$. These coherent oscillations transform the energy originally stored in the axion field into physical axion quanta. The contribution of this mechanism to the present axion relic density is [1]

$$\Omega_a h^2 = \kappa_a \left( f_a / 10^{12} \text{ GeV} \right)^{1.175} \theta_i^2 \ , \tag{24.5}$$

where the numerical factor $\kappa_a$ lies roughly between 0.5 and a few. If $\theta_i \sim \mathcal{O}(1)$, Eq. (24.5) will saturate Eq. (24.1) for $f_a \sim 10^{11}$ GeV, comfortably above laboratory and astrophysical constraints [10]; this would correspond to an axion mass around 0.1 meV. However, if the post-inflationary reheat temperature $T_R > f_a$, cosmic strings will form during the PQ phase transition at $T \simeq f_a$. Their decay will give an additional contribution to $\Omega_a$, which is often bigger than that in Eq. (24.5) [1], leading to a smaller preferred value of $f_a$, *i.e.*, larger $m_a$. On the other hand, values of $f_a$ near the Planck scale become possible if $\theta_i$ is for some reason very small.

"Sterile" $SU(2) \times U(1)_Y$ singlet neutrinos with keV masses [11] could alleviate the "cusp/core problem" [1] of cold DM models. If they were produced non-thermally through mixing with standard neutrinos, they would eventually decay into a standard neutrino and a photon.

Weakly interacting massive particles (WIMPs) $\chi$ are particles with mass roughly between 10 GeV and a few TeV, and with cross sections of approximately weak strength. Within standard cosmology, their present relic density can be calculated reliably if the WIMPs were in thermal and chemical equilibrium with the hot "soup" of Standard Model (SM) particles after inflation. In this case, their density would become exponentially (Boltzmann) suppressed at $T < m_\chi$. The WIMPs therefore drop out of thermal equilibrium ("freeze out") once the rate of reactions that change SM particles into WIMPs or vice versa, which is proportional to the product of the WIMP number density and the WIMP pair annihilation cross section into SM particles $\sigma_A$ times velocity, becomes smaller than the Hubble expansion rate of the Universe. After freeze out, the co-moving WIMP density remains essentially constant; if the Universe evolved adiabatically after WIMP decoupling, this implies a constant WIMP number to entropy density ratio. Their present relic density is then approximately given by (ignoring logarithmic corrections) [12]

$$\Omega_\chi h^2 \simeq const. \cdot \frac{T_0^3}{M_{\rm Pl}^3 \langle \sigma_A v \rangle} \simeq \frac{0.1 \text{ pb} \cdot c}{\langle \sigma_A v \rangle} \ . \tag{24.6}$$

Here $T_0$ is the current CMB temperature, $M_{\rm Pl}$ is the Planck mass, $c$ is the speed of light, $\sigma_A$ is the total annihilation cross section of a pair of WIMPs into SM particles, $v$ is the relative velocity between the two WIMPs in their cms system, and $\langle \ldots \rangle$ denotes thermal averaging. Freeze out happens at temperature $T_F \simeq m_\chi/20$ almost independently of the properties of the WIMP. This means that WIMPs are already non-relativistic when they decouple from the thermal plasma; it also implies that Eq. (24.6) is applicable if $T_R > T_F$. Notice that the 0.1 pb in Eq. (24.6) contains factors of $T_0$ and $M_{\rm Pl}$; it is, therefore, quite

intriguing that it "happens" to come out near the typical size of weak interaction cross sections.

The seemingly most obvious WIMP candidate is a heavy neutrino. However, an SU(2) doublet neutrino will have too small a relic density if its mass exceeds $M_Z/2$, as required by LEP data. One can suppress the annihilation cross section, and hence increase the relic density, by postulating mixing between a heavy SU(2) doublet and some sterile neutrino. However, one also has to require the neutrino to be stable; it is not obvious why a massive neutrino should not be allowed to decay.

The currently best motivated WIMP candidate is, therefore, the lightest superparticle (LSP) in supersymmetric models [13] with exact R-parity (which guarantees the stability of the LSP). Searches for exotic isotopes [14] imply that a stable LSP has to be neutral. This leaves basically two candidates among the superpartners of ordinary particles, a sneutrino, and a neutralino. The negative outcome of various WIMP searches (see below) rules out "ordinary" sneutrinos as primary component of the DM halo of our galaxy. The most widely studied WIMP is therefore the lightest neutralino. Detailed calculations [1] show that the lightest neutralino will have the desired thermal relic density Eq. (24.1) in at least four distinct regions of parameter space. $\chi$ could be (mostly) a bino or photino (the superpartner of the $U(1)_Y$ gauge boson and photon, respectively), if both $\chi$ and some sleptons have mass below $\sim 150$ GeV, or if $m_\chi$ is close to the mass of some sfermion (so that its relic density is reduced through co-annihilation with this sfermion), or if $2m_\chi$ is close to the mass of the *CP*-odd Higgs boson present in supersymmetric models. Finally, Eq. (24.1) can also be satisfied if $\chi$ has a large higgsino or wino component.

Many non-supersymmetric extensions of the Standard Model also contain viable WIMP candidates [1]. Examples are the lightest $T-$odd particle in "Little Higgs" models with conserved $T-$parity, or "techni-baryons" in scenarios with an additional, strongly interacting ("technicolor" or similar) gauge group.

There also exist models where the DM particles, while interacting only weakly with ordinary matter, have quite strong interactions within an extended "dark sector" of the theory. These were motivated by measurements by the PAMELA, ATIC and FERMI satellites indicating excesses in the cosmic $e^+$ and/or $e^-$ fluxes at high energies. However, these excesses are relative to background estimates that are clearly too simplistic (*e.g.*, neglecting primary sources of electrons and positrons, and modeling the galaxy as a homogeneous cylinder). Moreover, the excesses, if real, are far too large to be due to usual WIMPs, but can be explained by astrophysical sources. It therefore seems unlikely that they are due to Dark Matter [15]. Similarly, claims of positive signals for direct WIMP detection by the DAMA and, more recently, CoGeNT and CRESST collaborations (see below) led to the development of tailor-made models to alleviate tensions with null experiments. Since we are not convinced that these data indeed signal WIMP detection, and these models (some of which were quickly excluded by improved measurements) lack independent motivation, we will not discuss them any further in this Review.

Although thermally produced WIMPs are attractive DM candidates because their relic density naturally has at least the right order of magnitude, non-thermal production mechanisms have also been suggested, *e.g.*, LSP production from the decay of some moduli fields [16], from the decay of the inflaton [17], or from the decay of "$Q-$balls"

(non-topological solitons) formed in the wake of Affleck-Dine baryogenesis [18]. Although LSPs from these sources are typically highly relativistic when produced, they quickly achieve kinetic (but not chemical) equilibrium if $T_R$ exceeds a few MeV [19]( but stays below $m_\chi/20$). They therefore also contribute to cold DM. Finally, if the WIMPs aren't their own antiparticles, an asymmetry between WIMPs and antiWIMPs might have been created in the early Universe, possibly by the same (unknown) mechanism that created the baryon antibaryon asymmetry. In such "asymmetric DM" models [20] the WIMP antiWIMP annihilation cross section $\langle\sigma_A v\rangle$ should be significantly larger than $1\,\mathrm{pb}\cdot c$, cf Eq. (24.6).

The absence of signals at the LHC for physics beyond the Standard Model, as well as the discovery of an SM-like Higgs boson with mass near 126 GeV, constrains many well-motivated WIMP models. For example, in constrained versions of the minimal supersymmetrized Standard Model (MSSM) both the absence of supersymmetric signals and the relatively large mass of the Higgs boson favor larger WIMP masses and lower scattering cross sections on nucleons. However, constraints from "new physics" searches apply most directly to strongly interacting particles. Many WIMP models therefore can still accommodate a viable WIMP for a wide range of masses. For example, in supersymmetric models where the bino mass is not related to the other gaugino masses a bino with mass as small as 15 GeV can still have the correct thermal relic density [21]. Even lighter supersymmetric WIMPs can be realized in models with extended Higgs sector [22].

Primary black holes (as MACHOs), axions, sterile neutrinos, and WIMPs are all (in principle) detectable with present or near-future technology (see below). There are also particle physics DM candidates which currently seem almost impossible to detect, unless they decay; the present lower limit on their lifetime is of order $10^{25}$ to $10^{26}$ s for 100 GeV particles. These include the gravitino (the spin-3/2 superpartner of the graviton), states from the "hidden sector" thought responsible for supersymmetry breaking, and the axino (the spin-1/2 superpartner of the axion) [1].

## 24.2. Experimental detection of Dark Matter

### 24.2.1. *The case of baryonic matter in our galaxy* :

The search for hidden galactic baryonic matter in the form of MAssive Compact Halo Objects (MACHOs) has been initiated following the suggestion that they may represent a large part of the galactic DM and could be detected through the microlensing effect [4]. The MACHO, EROS, and OGLE collaborations have performed a program of observation of such objects by monitoring the luminosity of millions of stars in the Large and Small Magellanic Clouds for several years. EROS concluded that MACHOs cannot contribute more than 8% to the mass of the galactic halo [23], while MACHO observed a signal at 0.4 solar mass and put an upper limit of 40%. Overall, this strengthens the need for non-baryonic DM, also supported by the arguments developed above.

### 24.2.2. *Axion searches* :

Axions can be detected by looking for $a \to \gamma$ conversion in a strong magnetic field [1]. Such a conversion proceeds through the loop-induced $a\gamma\gamma$ coupling, whose strength $g_{a\gamma\gamma}$ is an important parameter of axion models. There is currently only one experiment searching for axionic DM: the ADMX experiment [30], originally situated at the LLNL in California but now running at the University of Washington, started taking data in the first half of 1996. It employs a high quality cavity, whose "Q factor" enhances the conversion rate on resonance, *i.e.*, for $m_a(c^2 + v_a^2/2) = \hbar\omega_{\rm res}$. One then needs to scan the resonance frequency in order to cover a significant range in $m_a$ or, equivalently, $f_a$. ADMX now uses SQUIDs as first-stage amplifiers; their extremely low noise temperature (1.2 K) enhances the conversion signal. Published results [24], combining data taken with conventional amplifiers and SQUIDs, exclude axions with mass between 1.9 and 3.53 $\mu$eV, corresponding to $f_a \simeq 4 \cdot 10^{13}$ GeV, for an assumed local DM density of 0.45 GeV/cm$^3$, if $g_{a\gamma\gamma}$ is near the upper end of the theoretically expected range. About five times better limits on $g_{a\gamma\gamma}$ were achieved [25] for 1.98 $\mu$eV $\leq m_a \leq$ 2.18 $\mu$eV as well as for 3.3 $\mu$eV $\leq m_a \leq$ 3.65 $\mu$eV, if a large fraction of the local DM density is due to a single flow of axions with very low velocity dispersion. The ADMX experiment is being upgraded by reducing the cavity and SQUID temperature from the current 1.2 K to about 0.1 K. This should increase the frequency scanning speed for given sensitivity by more than two orders of magnitude, or increase the sensitivity for fixed observation time.

### 24.2.3. *Searches for keV Neutrinos* :

Relic keV neutrinos $\nu_s$ can only be detected if they mix with the ordinary neutrinos. This mixing leads to radiative $\nu_s \to \nu\gamma$ decays, with lifetime $\tau_{\nu_s} \simeq 1.8 \cdot 10^{21}$ s $\cdot (\sin\theta)^{-2} \cdot (1\ {\rm keV}/m_{\nu_s})^5$, where $\theta$ is the mixing angle [11]. This gives rise to a flux of mono-energetic photons with $E_\gamma = m_{\nu_s}/2$, which might be observable by *X-ray* satellites. In the simplest case the relic $\nu_s$ are produced only by oscillations of standard neutrinos. Assuming that all lepton-antilepton asymmetries are well below $10^{-3}$, the $\nu_s$ relic density can then be computed uniquely in terms of the mixing angle $\theta$ and the mass $m_{\nu_s}$. The combination of lower bounds on $m_{\nu_s}$ from analyses of structure formation (in particular, the Ly$\alpha$ "forest") and upper bounds on *X-ray* fluxes from various (clusters of) galaxies exclude this scenario if $\nu_s$ forms all of DM. This conclusion can be evaded if $\nu_s$ forms only part of DM, and/or if there is a lepton asymmetry $\geq 10^{-3}$ (i.e. some 7 orders of magnitude above the observed baryon-antibaryon asymmetry), and/or if there is an additional source of $\nu_s$ production in the early Universe, e.g. from the decay of heavier particles [11].

### 24.2.4. *Basics of direct WIMP search* :

As stated above, WIMPs should be gravitationally trapped inside galaxies and should have the adequate density profile to account for the observed rotational curves. These two constraints determine the main features of experimental detection of WIMPs, which have been detailed in the reviews in [1].

Their mean velocity inside our galaxy relative to its center is expected to be similar to that of stars, *i.e.*, a few hundred kilometers per second at the location of our solar system.

For these velocities, WIMPs interact with ordinary matter through elastic scattering on nuclei. With expected WIMP masses in the range 10 GeV to 10 TeV, typical nuclear recoil energies are of order of 1 to 100 keV.

The shape of the nuclear recoil spectrum results from a convolution of the WIMP velocity distribution, usually taken as a Maxwellian distribution in the galactic rest frame, shifted into the Earth rest frame, with the angular scattering distribution, which is isotropic to first approximation but forward-peaked for high nuclear mass (typically higher than Ge mass) due to the nuclear form factor. Overall, this results in a roughly exponential spectrum. The higher the WIMP mass, the higher the mean value of the exponential. This points to the need for low nuclear recoil energy threshold detectors.

On the other hand, expected interaction rates depend on the product of the local WIMP flux and the interaction cross section. The first term is fixed by the local density of dark matter, taken as 0.39 GeV/cm$^3$ [see Eq. (24.3)], the mean WIMP velocity, typically 220 km/s, the galactic escape velocity, typically 544 km/s [26] and the mass of the WIMP. The expected interaction rate then mainly depends on two unknowns, the mass and cross section of the WIMP (with some uncertainty [6] due to the halo model). This is why the experimental observable, which is basically the scattering rate as a function of energy, is usually expressed as a contour in the WIMP mass–cross section plane.

The cross section depends on the nature of the couplings. For non-relativistic WIMPs, one in general has to distinguish spin-independent and spin-dependent couplings. The former can involve scalar and vector WIMP and nucleon currents (vector currents are absent for Majorana WIMPs, *e.g.*, the neutralino), while the latter involve axial vector currents (and obviously only exist if $\chi$ carries spin). Due to coherence effects, the spin-independent cross section scales approximately as the square of the mass of the nucleus, so higher mass nuclei, from Ge to Xe, are preferred for this search. For spin-dependent coupling, the cross section depends on the nuclear spin factor; used target nuclei include $^{19}$F, $^{23}$Na, $^{73}$Ge, $^{127}$I, $^{129}$Xe, $^{131}$Xe, and $^{133}$Cs.

Cross sections calculated in MSSM models [27] induce rates of at most 1 evt day$^{-1}$ kg$^{-1}$ of detector, much lower than the usual radioactive backgrounds. This indicates the need for underground laboratories to protect against cosmic ray induced backgrounds, and for the selection of extremely radio-pure materials.

The typical shape of exclusion contours can be anticipated from this discussion: at low WIMP mass, the sensitivity drops because of the detector energy threshold, whereas at high masses, the sensitivity also decreases because, for a fixed mass density, the WIMP flux decreases $\propto 1/m_\chi$. The sensitivity is best for WIMP masses near the mass of the recoiling nucleus.

Two important points are to be kept in mind when comparing exclusion curves from various experiments between them or with positive indications of a signal.

For an experiment with a fixed nuclear recoil energy threshold, the lower is the considered WIMP mass, the lower is the fraction of the spectrum to which the experiment is sensitive. This fraction may be extremely small in some cases. For instance CoGeNT [28], using a Germanium detector with an energy threshold of around 2 keV, is sensitive to about 10 % of the total recoil spectrum of a 7 GeV WIMP, while for

XENON100 [29], using a liquid Xenon detector with a threshold of 8.4 keV, this fraction is only 0.05 % (that is the extreme tail of the distribution), for the same WIMP mass. The two experiments are then sensitive to very different parts of the WIMP velocity distribution.

A second important point to consider is the energy resolution of the detector. Again at low WIMP mass, the expected roughly exponential spectrum is very steep and when the characteristic energy of the exponential becomes of the same order as the energy resolution, the energy smearing becomes important. In particular, a significant fraction of the expected spectrum below effective threshold is smeared above threshold, increasing artificially the sensitivity. For instance, a Xenon detector with a threshold of 8 keV and infinitely good resolution is actually insensitive to a 7 GeV mass WIMP, because the expected energy distribution has a cut-off at roughly 5 keV. When folding in the experimental resolution of XENON100 (corresponding to a photostatistics of 0.5 photoelectron per keV), then around 1 % of the signal is smeared above 5 keV and 0.05 % above 8 keV. Setting reliable cross section limits in this mass range thus requires a complete understanding of the response of the detector at energies well below the nominal threshold.

In order to homogenize the reliability of the presented exclusion curves, and save the reader the trouble of performing tedious calculations, we propose to set cross section limits only for WIMP mass above a *"WIMP safe"* minimal mass value defined as the maximum of 1) the mass where the increase of sensitivity from infinite resolution to actual experimental resolution is not more than a factor two, and 2) the mass where the experiment is sensitive to at least 1 % of the total WIMP signal recoil spectrum. These recommendations are irrespective of the content of the experimental data obtained by the experiments.

Two experimental signatures are predicted for WIMP signals. One is a strong daily forward/backward asymmetry of the nuclear recoil direction, due to the alternate sweeping of the WIMP cloud by the rotating Earth. Detection of this effect requires gaseous detectors or anisotropic response scintillators (stilbene). The second is a few percent annual modulation of the recoil rate due to the Earth speed adding to or subtracting from the speed of the Sun. This tiny effect can only be detected with large masses; nuclear recoil identification should also be performed, as the otherwise much larger background may also be subject to seasonal modulation.

### 24.2.5. *Status and prospects of direct WIMP searches* :

Given the intense activity of the field, readers interested in more details than the ones given below may refer to [1], as well as to presentations at recent conferences [30].

The first searches have been performed with ultra-pure semiconductors installed in pure lead and copper shields in underground environments. Combining a priori excellent energy resolutions and very pure detector material, they produced the first limits on WIMP searches (Heidelberg-Moscow, IGEX, COSME-II, HDMS) [1]. Planned experiments using several tens of kg to a ton of Germanium run at liquid nitrogen temperature (designed for double-beta decay search) – GERDA, MAJORANA – are based in addition on passive reduction of the external and internal electromagnetic and

neutron background by using Point Contact detectors (discussed below), minimal detector housing, close electronics, pulse shape discrimination and large liquid nitrogen or argon shields. Their sensitivity to WIMP interactions will depend on their ability to lower the energy threshold sufficiently, while keeping the background rate small.

Great progress has recently been made in the development of so called Point Contact Germanium detectors, with a very small capacitance allowing one to reach sub-keV thresholds. The CoGeNT collaboration was first operating a single 440 g Germanium detector with an effective threshold of 400 eV in the Soudan Underground Laboratory for 56 days [28]. After applying a rise time cut on the pulse shapes in order to remove the surface interactions known to suffer from incomplete charge collection, the resulting spectrum below 4 keV is said by the authors to exhibit an irreducible excess of events, with energy spectrum roughly exponential, compatible with a light WIMP with mass in the 7 to 11 GeV range, and cross section around $10^{-4}$ pb. The most recent published result [31] claims the presence of a signal, compatible with WIMPs in the same mass range but with a lower central cross section of $3 \times 10^{-5}$ pb.

However, at energies around 1 keV where this signal is claimed to reside, the bulk and surface event populations show overlapping rise time distributions. According to the TEXONO [32] and MALBEK [33] collaborations, this makes an accurate separation of these populations very difficult. Additional confusion has been added by the multiplicity of "regions of interest" published by the CoGeNT collaboration and in other analyses [34].

Results [35] based on data accumulated by CoGeNT during one year led to the claim of a modulated signal. However, the modulation is much stronger than expected from a standard WIMP. Moreover, CDMS has similar sensitivity but sees no modulation [36].

The new CDEX/TEXONO consortium plans to build a 10 kg array of small Ge detectors with a claimed very low (100 eV) threshold, and to operate them in the new Chinese Jinping underground laboratory, the deepest in the world. Such a detector would be sensitive to all recently claimed "signal regions" or "regions of interest" of $\sim 10$ GeV WIMPs.

In order to make progress in the reliability of any claimed signal, active background rejection and signal identification questions have to be addressed. Active background rejection in detectors relies on the relatively small ionization in nuclear recoils due to their low velocity. This induces a reduction ("quenching") of the ionization/scintillation signal for nuclear recoil signal events relative to $e$ or $\gamma$ induced backgrounds. Energies calibrated with gamma sources are then called "electron equivalent energies" (keVee unit used below). This effect has been both calculated and measured [1]. It is exploited in cryogenic detectors described later. In scintillation detectors, it induces in addition a difference in decay times of pulses induced by $e/\gamma$ events vs nuclear recoils. In most cases, due to the limited resolution and discrimination power of this technique at low energies, this effect allows only a statistical background rejection. It has been used in NaI(Tl) (DAMA, LIBRA, NAIAD, Saclay NaI), in CsI(Tl) (KIMS), and Xe (ZEPLIN-I) [1,30]. Pulse shape discrimination is particularly efficient in liquid argon. Using a high energy threshold, it has been used for an event by event discrimination by the WARP experiment, but the high threshold led to a moderate signal sensitivity. No observation of nuclear recoils has been reported by any of these experiments.

The DAMA collaboration has reported results from a total of 6 years exposure with the LIBRA phase involving 250 kg of detectors, plus the earlier 6 years exposure of the original DAMA/NaI experiment with 100 kg of detectors [37], for a cumulated exposure of 1.17 t·y. They observe an annual modulation of the signal in the 2 to 6 keVee bin, with the expected period (1 year) and phase (maximum around June 2), at 8.9 $\sigma$ level. If interpreted within the standard halo model described above, two possible explanations have been proposed: a WIMP with $m_\chi \simeq 50$ GeV and $\sigma_{\chi p} \simeq 7 \cdot 10^{-6}$ pb (central values) or at low mass, in the 6 to 10 GeV range with $\sigma_{\chi p} \sim 10^{-3}$ pb; the cross section could be somewhat lower if there is a significant channeling effect [1].

Interpreting these observations as positive WIMP signal raises several issues of internal consistency. First, the proposed WIMP solutions would induce a sizeable fraction of nuclear recoils in the total measured rate in the 2 to 6 keVee bin. No pulse shape analysis has been reported by the authors to check whether the unmodulated signal was detectable this way. Secondly, the residual $e/\gamma$-induced background, inferred by subtracting the signal predicted by the WIMP interpretation from the data, has an unexpected shape [38], starting near zero at threshold and quickly rising to reach its maximum near 3 to 3.5 keVee; from general arguments one would expect the background (e.g. due to electronic noise) to increase towards the threshold. Finally, the amplitude of the annual modulation shows a somewhat troublesome tendency to decrease with time. The original DAMA data, taken 1995 to 2001, gave an amplitude of the modulation of $20.0 \pm 3.2$ in units of $10^{-3}$ counts/(kg·day·keVee), in the 2-6 keVee bin. During the first phase of DAMA/LIBRA, covering data taken between 2003 and 2007, this amplitude became $10.7 \pm 1.9$, and in the second phase of DAMA/LIBRA, covering data taken between 2007 and 2009, it further decreased to $8.5 \pm 2.2$. The ratio of amplitudes inferred from the DAMA/LIBRA phase 2 and original DAMA data is $0.43 \pm 0.13$, differing from the expected value of 1 by more than 4 standard deviations. (The results for the DAMA/LIBRA phase 2 have been calculated by us using published results for the earlier data alone [39] as well as for the latest grand total [37]. ) Similar conclusions can be drawn from analyses of the 2-4 and 2-5 keVee bins.

Concerning compatibility with other experiments (see below), the high mass solution is clearly excluded by many null observations, while possibly a small parameter space remains available for the low mass solution (according to [38] this possibility is excluded if the energy spectrum measured by DAMA/LIBRA is taken into account). It should be noted that these comparisons have to make assumptions about the WIMP velocity distribution (see above), but varying this within reasonable limits does not resolve the tension [38]. Moreover, one usually assumes that the WIMP scatters elastically, and that the spin-independent cross section for scattering off protons and neutrons is roughly the same. These assumptions are satisfied by all models we know that are either relatively simple (i.e. do not introduce many new particles) or have independent motivation (e.g. attempting to solve the hierarchy problem). As noted earlier, models have been constructed where these assumptions do not hold, but at least some of these are no longer able to make the WIMP interpretation of the DAMA(/LIBRA) observations compatible with all null results from other experiments. Finally, appealing to spin-dependent interactions does not help, either [40], in view of null results from

direct searches as well as limits on neutrino fluxes from the Sun (see the subsection on indirect WIMP detection below).

KIMS [41], an experiment operating 12 crystals of CsI(Tl) with a total mass of 104.4 kg in the Yang Yang (renamed CUNP) laboratory in Korea, has given an upper limit on nuclear recoils present in a 24 t·d exposure. This translates into an upper limit on the cross section roughly two orders of magnitude below that required to explain the DAMA signal by a 60 GeV WIMP. It should be noted that these results are directly comparable as they involve the same nucleus (I). Based on a modulation analysis of 2.5 years of continuous operation which failed to find a signal, the KIMS collaboration very recently announced [42] preliminary results which exclude the high mass solution and most of the low mass WIMP explanation of DAMA signal.

ANAIS [30], a 100 kg NaI(Tl) project planned to be run at the Canfranc lab, is in the phase of crystal selection and purification. DM-ice is a new project with the aim of checking the DAMA/LIBRA modulation signal in the southern hemisphere. It will consist of 250 kg of NaI(Tl) installed in the heart of the IceCube array. The counting rate of crystals from the previous NAIAD array recently measured in situ is currently dominated by internal radioactivity.

At mK temperature, the simultaneous measurement of the phonon and ionization signals in semiconductor detectors permits event by event discrimination between nuclear and electronic recoils down to 5 to 10 keV recoil energy. This feature is being used by the CDMS [30] and EDELWEISS [30] collaborations. Surface interactions, exhibiting incomplete charge collection, are an important residual background, which has been treated so far by two different techniques: CDMS uses the timing information of the phonon pulse, while EDELWEISS uses the ionization pulses in an interleaved electrodes scheme. In 2011 CDMS published [43] results using 19 Germanium cryogenic detectors at the Soudan mine involving a total exposure of around 612 kg·d (around 300 kg·d fiducial); they exclude spin-independent WIMP nucleon cross sections above $3.8 \times 10^{-8}$ pb, at 90% CL for a 70 GeV WIMP.

The recent announcement [44] of a possible excess of events in data obtained with the CDMS Silicon detectors drew particular attention. They found three events after cuts in a blind analysis of 140 kg·d exposure obtained with eight Silicon detectors run in 2007-2008. While the expected background of 0.7 events lead to a 5 % probability for the three events to be background based on the number of events alone, the phonon rise time and ionization yield values of the three events appear perfectly compatible with nuclear recoils, giving a total probability of 0.19 % that they are due to known background from a profile likelihood ratio test. The best fit yields a cross section $\sim 10^{-7}$ pb and a WIMP mass of 8 GeV. The corresponding 90 % confidence contour has some overlap with the "region of interest" claimed by CoGeNT.

However, the case made by CDMS is weakened by 1) the very close proximity of the strength of the ionization signal of all three events to the cut, 2) the simultaneous publication by the same collaboration of a second paper on an independent set of 56 kg·d Silicon data with no events observed and an estimated background of 1.1 events [45]. One would like to see a combined analysis, and how the population of events surviving a relaxed cut on ionization energy behaves in rise time and ionization yield.

Very recently, CDMS has reported [46] the result of the analysis of a data set named CDMS-Lite obtained by running a single detector in a particular mode allowing an equivalent electron energy threshold of 270 eV. This is obtained by applying a high voltage (69 V) across the ionization measurement electrodes. The phonons then generated by the ionization electrons traveling inside the crystal – so called Neganov Luke effect – largely overcome the normal induced phonon pulse by the initial interaction. This amplifies the ionization pulse, but no discrimination between electron and nuclear recoils is possible in this mode. The sensitivity is then fixed by the counting rate at threshold, and could be anticipated from a downward extrapolation of the background above 1.5 keV. An interesting rejection curve is obtained, quite flat for WIMP masses between 6 to 12 GeV, and rather insensitive to the systematic uncertainty on the quenching factor. It cuts the latest CoGeNT "region of interest" in the middle and lies a factor 1.8 above the central value of the CDMS Si result.

Results of a run using 9 kg of new detectors fitted with interleaved electrodes and operated in Soudan mine since November 2011 are expected by the end of 2013.

The EDELWEISS collaboration [30], which operates Germanium cryogenic detectors in the Laboratoire Souterrain de Modane, has reported a low energy analysis [47], with a similar principle to the CDMS low energy analysis of 2011 [48]. The exclusion curve happens to complement the gap in sensitivity in the CDMS limits for WIMP masses between 8 and 10 GeV, precisely a factor 3 above the central value of the CDMS-Si result (see above).

EDELWEISS is assembling new 800 g detectors featuring a complete coverage of the crystal with annular electrodes, and better rejection of non-recoil events. Around 30 kg of these detectors are expected to be operated inside an improved cryostat starting in 2014.

The combined analysis of CDMS and EDELWEISS data [49] currently gives the second best limit on the SI cross sections for WIMPS masses above 80 GeV.

The cryogenic experiment CRESST [30] in the Gran Sasso laboratory uses the scintillation of $CaWO_4$ as second variable for background discrimination. In their analysis of 730 kg·d exposure they reported [50] the observation of 67 events in the signal region, where about 40 background events were expected. The event excess is said to be compatible with WIMP scattering. A likelihood method provides two solutions, respectively for WIMPs with mass 12 and 25 GeV. The size of the signal (if any) hinges on the reliability of the background model, which has to account for several classes of background whose properties bracket those of the signal. New detectors, with hopefully reduced backgrounds and better coverage of the scintillating layer allowing the identification of $\alpha$ particles, are being operated.

The next stages of solid state detectors, SuperCDMS and EURECA-I (a combination of EDELWEISS and CRESST), will involve typically 150 kg to 200 kg of detectors. Various presentations at conferences indicate that these two collaborations are working on a possible merger to a common project.

Noble gas detectors for dark matter detection are being actively developed by several groups [1]. Dual (liquid and gas) phase detectors allow to measure both the primary scintillation and the ionization electrons drifted through the liquid and amplified in the

gas, which is used for background rejection.

The XENON collaboration [30] operates the 161 kg XENON100 setup at Gran Sasso laboratory. It has published a result [29] based on 225 days of operating time. Within a fiducial mass of 34 kg, two events were observed in the signal region, while 1.0 were expected. The obtained minimum cross section for spin-independent interactions is $2.0 \times 10^{-9}$ pb for a mass of 55 GeV. The reliability of limits set at masses lower than 12 GeV, especially with respect to the relative light efficiency factor, have been discussed in the community. Moreover, as underlined near the end of section 1.2.4, the limits at low mass can be set *only* thanks to the poor energy resolution at threshold – 8.4 keV – due to the low photoelectron yield of 0.5 pe/keV. With infinite energy resolution, a Xe detector *with the same threshold of 8.4 keV* is not sensitive to a WIMP mass of 7 GeV. The *"WIMP safe"* minimal mass for XENON100 is around 12 GeV. This data set provides the best limit for spin dependent WIMPs with pure neutron couplings at all masses [51].

A reanalysis of part of the XENON10 data [52], using the ionization signal only, with an ionization yield of around 3.5 electron/keV at a threshold of 1.4 keV, sets a more stringent limit for WIMP masses below 12 GeV. The *"WIMP safe"* minimal mass for this XENON10 analysis is around 5 GeV. However, a reanalysis of the data [53] showed that the published limit was too strong. The authors acknowledged this error.

XENON1t, the successor of XENON100 again planned to be run at the Gran Sasso lab, is starting construction.

The ZEPLIN III experiment [30], using a dual phase Xenon detector with an active mass of 12 kg, operated in the Boulby laboratory. It published final results with an exposure of 1344 kg·d [54]. This provides the second best limit for SD interactions on neutrons. The limits on SI interactions are comparable to those from CDMS and EDELWEISS. This experiment has ended.

A new liquid Xenon based project, PANDA-X, with pancake geometry, planned to be housed in the new Jinping lab, will start operating soon.

The LUX detector [30], a 370 kg double phase Xenon detector installed in a large water shield, is being operated in the new SURF (previous Homestake) laboratory in US. The LUX collaboration has recently announced [55]( results not published at the edition time of this review) results from an 85 days run, with a fiducial mass of 118 kg . Thanks to an extremely low content of $^{85}$Kr (5 times lower than in Xenon100) and a very good light collection efficiency of 14 %, they could reach unprecedented sensitivity both at high and low mass WIMP's. After cuts, they observed 160 events inside the fiducial volume, in the nuclear recoil energy window of roughly 4 to 27 keV. A profile likelihood ratio analysis shows that the discrimination parameter versus scintillation energy scatter plot is compatible with a pure population of electron events, with upper limits on the presence of nuclear recoils ranging from 2.4 to 5.3 events, depending on the WIMP mass. This allowed LUX to set the best lower limit on the cross section for spin-independent interactions at $7.6 \times 10^{-10}$ pb for a 33 GeV WIMP mass. Limits in the range 7 to 8 GeV are between a factor 100 and 1000 lower than the cross section of the CoGeNT and CDMS-Silicon "regions of interest". It should be kept in mind however that the *"WIMP safe"* minimal mass" for this LUX data set is around 8-10 GeV. The fraction of WIMP

signal (and thus WIMP velocities) probed by LUX at around 8 GeV is less than a few $10^{-3}$ (that is the highest WIMP velocity tail) while it is a few $10^{-2}$ for the CDMS-Silicon data and few $10^{-1}$ for CoGeNT data.

XMASS [30] in Japan has taken first data with a single-phase 800 kg Xenon detector (100 kg fiducial mass, allowing a strong self shielding) installed in a large pure water shield at the SuperKamiokande site. Unfortunately a strong radioactive contamination of some aluminum pieces of the detector was found in the first run. The detector is being upgraded with radiopure materials.

The ArDM project [30] is a double phase Argon detector with a total mass of 1,100 kg. It will soon take data at the Canfranc laboratory. MiniCLEAN and DEAP-3600 [30], both measuring only scintillation signals in spherical geometries in single phase mode, are being assembled at SNOLab and will operate respectively 500 kg of Ar/Ne and 3600 kg of Ar [1]. DarkSide [30] is another Argon based, double phase project, beginning with about 50 kg of $^{39}$Ar depleted Argon, to be operated from 2014 in the Gran Sasso lab.

The low pressure Time Projection Chamber technique is currently the only convincing way to measure the direction of nuclear recoils and prove the galactic origin of a possible signal [1]. The DRIFT collaboration [30] has operated a 1 m$^3$ volume detector filled with CS2 in the UK Boulby mine. The target mass is too small to probe WIMP models not already excluded by other experiments. The MIMAC collaboration [30], investigating a low pressure TPC detector, has published numerous papers on expected performances. A 2.5 l 1000 channel prototype has been operated in the Fréjus laboratory, with no new results yet. Other groups developing similar techniques, though with lower sensitivity, are DMTPC in the US and NewAge in Japan.

The following more unconventional detectors based on metastable liquids or gels, with the advantage to be insensitive to electromagnetic interactions and the drawback of being threshold yes/no detectors, were initially using compounds rich in $^{19}$F nucleus in order to set limits on the spin dependent coupling of WIMPs, with less than kg mass detectors. However, by varying the sensitive material and increasing the detector mass, they may also compete for SI interactions. The COUPP [30] collaboration using a 4 kg CF3I bubble chamber like detector, run at Fermilab, has published results [56] allowing them to set the best limit for spin dependent proton coupling at $3 \times 10^{-3}$ pb for a WIMP mass of 30 GeV. Picasso [30], a superheated droplet detector run at SNOLAB, obtained a better limit below 5 GeV on the same type of WIMPs [57]. SIMPLE [30], a similar experiment run at Laboratoire Souterrain de Rustrel, also produced competitive limits in an intermediate mass range [58].

PICO, combining the PICASSO and COUPP collaborations, is planning a dedicated detector, PICO2L, to search for light WIMPs, with mass between 1 and 10 GeV. Given the recent attractiveness of this mass range, several other experiments were proposed in the last couple of years, with the aim to operate less than 1 kg detectors with order of 0.1 keV energy threshold: DAMIC, using CCDs; and NEWS, using a spherical gaseous detector [42].

Figures 24.1 and 24.2 illustrate the limits on and positive claims for WIMP scattering cross sections, normalized to scattering on a single nucleon, for spin independent and spin

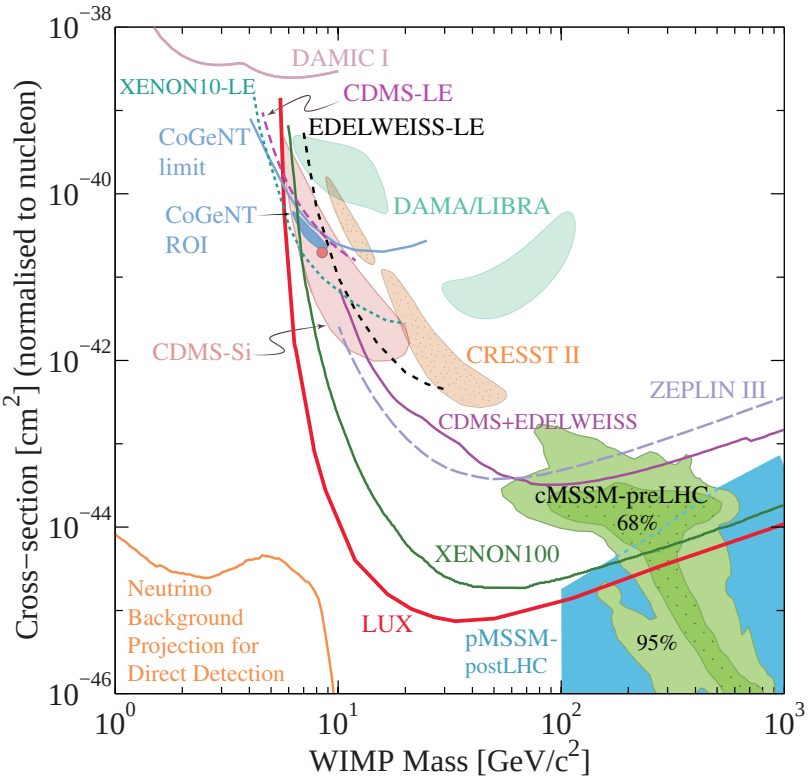


**Figure 24.1:** WIMP cross sections (normalized to a single nucleon) for spin-independent coupling versus mass. The DAMA/LIBRA [61], CREST II, CDMS-Si, and CoGeNT enclosed areas are regions of interest from possible signal events; the dot is the central value for CDMS-Si ROI. References to the experimental results are given in the text. For context, some supersymmetry implications are given: Green shaded 68% and 95% regions are pre-LHC cMSSM predictions by Ref. 62. Constraints set by XENON100 and the LHC experiments in the framework of the cMSSM [63] give regions in [300-1000 GeV; $1 \times 10^{-9} - 1 \times 10^{-12}$ pb] (but are not shown here). For the blue shaded region, pMSSM, an expansion of cMSSM with 19 parameters instead of 5 [64], also integrates constraints set by LHC experiments.

dependent couplings, respectively, as functions of WIMP mass. Only the two or three currently best limits are presented. Also shown are constraints from indirect observations (see the next section) and typical regions of SUSY models, before and after LHC results. These figures have been made with the `dmtools` web page, thanks to a nice new feature which allows to include new limits uploaded by the user into the plot [59].

Sensitivities down to $\sigma_{\chi p}$ of $10^{-13}$ pb, as needed to probe nearly all of the MSSM parameter space [27] at WIMP masses above 10 GeV and to saturate the limit of the irreducible neutrino-induced background [60], will be reached with detectors of multi ton masses, assuming nearly perfect background discrimination capabilities. Such experiments are envisaged by the US project LZ (6 tons), the European consortium DARWIN, and the MAX project (a liquid Xe and Ar multiton project). For WIMP masses below 10 GeV, this cross section limit is set by the solar neutrinos, inducing an

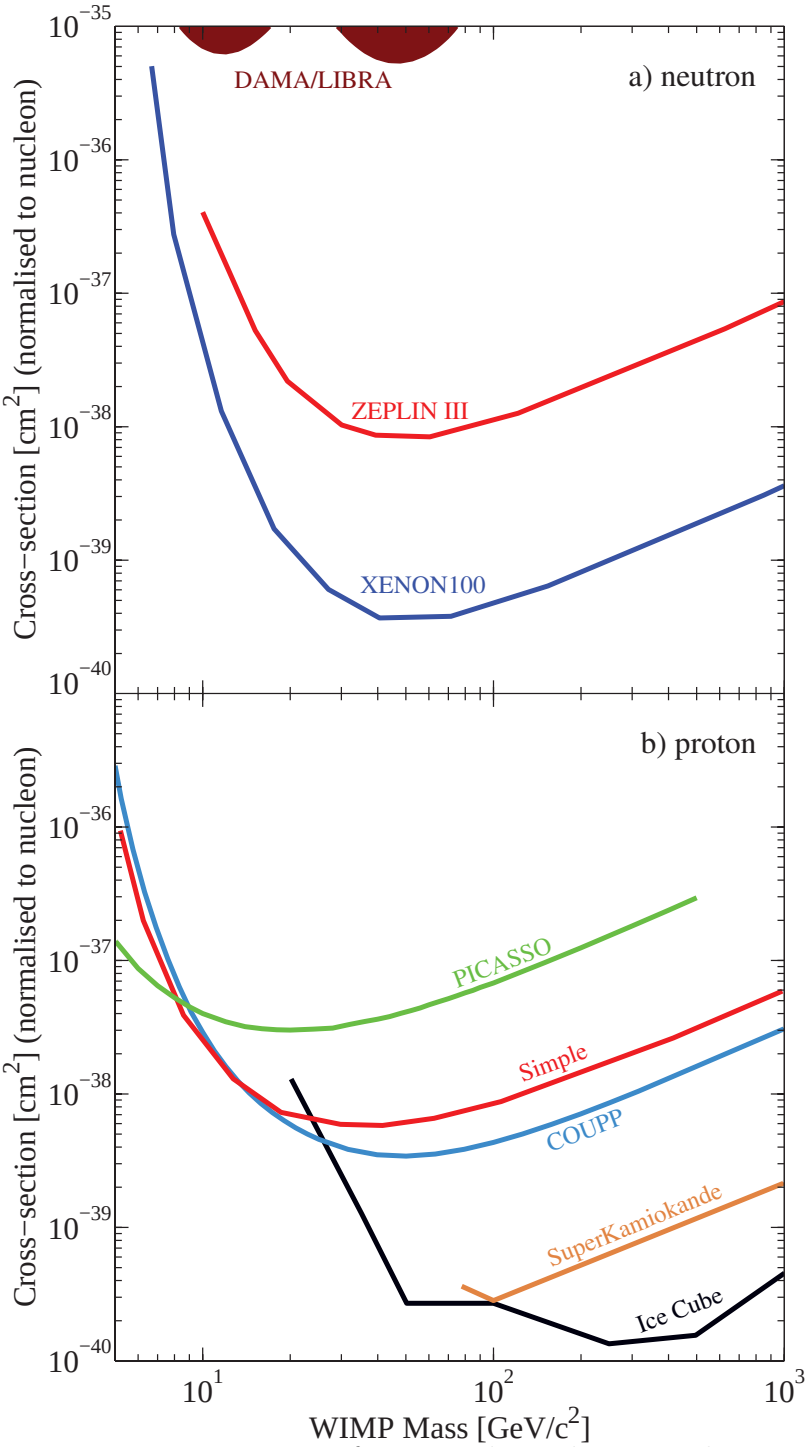


**Figure 24.2:** WIMP cross sections for spin dependent coupling versus mass. (a) interactions with the neutron; (b) interactions with the proton. References to the experimental results are given in the text. The limits quoted here from SuperKamiokande and IceCube assumes annihilation into $W^+W^-$. Assuming annihilation into $b\bar{b}$ gives softer neutrino spectrum and hence higher limits on the cross section, the better limit coming from SuperKamiokande at low mass. The limit quoted for COUPP assumes the most favorable bubble nucleation efficiency, The least favorable one gives a limit roughly 2 times higher.

irreducible background at an equivalent cross section around $10^{-9}$ pb, which in principle is accessible with less massive low threshold detectors [30].

### 24.2.6. *Status and prospects of indirect WIMP searches* :

WIMPs can annihilate and their annihilation products can be detected; these include neutrinos, gamma rays, positrons, antiprotons, and antinuclei [1]. These methods are complementary to direct detection and might be able to explore higher masses and different coupling scenarios. "Smoking gun" signals for indirect detection are GeV neutrinos coming from the center of the Sun or Earth, and monoenergetic photons from WIMP annihilation in space.

WIMPs can be slowed down, captured, and trapped in celestial objects like the Earth or the Sun, thus enhancing their density and their probability of annihilation. This is a source of muon neutrinos which can interact in the Earth. Upward going muons can then be detected in large neutrino telescopes such as MACRO, BAKSAN, SuperKamiokande, Baikal, AMANDA, ANTARES, NESTOR, and the large sensitive area IceCube [1]. The best upper limit for relatively soft muons comes from SuperKamiokande [30]. For example, the upper bound on the muon flux due to neutrinos from the Sun originating from a 50 GeV WIMP annihilating into $b\bar{b}$ pairs is about 1500 muons/km$^2$/year [65]. For more energetic muons the best bounds have been derived from a combination of AMANDA and IceCube40 data (i.e. data using 40 strings of the IceCube detector). For example, for a 1 TeV WIMP annihilating into $W^+W^-$ the upper bound on the muon flux is 103 muons/km$^2$/year [66]. In future data including the DeepCore array, which has become part of the completed IceCube detector, will likely dominate this field, possibly except at the very lowest muon energies. However, published bounds from DeepCore in combination with IceCube79 [67] are still weaker than those from SuperKamiokande for relatively soft muons, and are weaker than the combined AMANDA / IceCube40 bound for very energetic muons. For standard halo velocity profiles, only the limits from the Sun, which mostly probe spin-dependent couplings, are competitive with direct WIMP search limits.

WIMP annihilation in the halo can give a continuous spectrum of gamma rays and (at one-loop level) also monoenergetic photon contributions from the $\gamma\gamma$ and $\gamma Z$ channels. These channels also allow to search for WIMPs for which direct detection experiments have little sensitivity, *e.g.*, almost pure higgsinos. The size of this signal depends strongly on the halo model, but is expected to be most prominent near the galactic center. The central region of our galaxy hosts a strong TeV point source discovered [68] by the H.E.S.S. Cherenkov telescope [30]. Moreover, FERMI/LAT [30] data revealed a new extended source of GeV photons near the galactic center above and below the galactic plane [69]. Both of these sources are very likely of (mostly) astrophysical origin. The presence of these unexpected backgrounds makes it more difficult to discover WIMPs in this channel.

Nevertheless a feature has been found [70] in public FERMI/LAT data using a predetermined search region around the galactic center, where known point sources have been removed. Within the resolution of the detector this feature could be due to monoenergetic photons with energy $\sim 130$ GeV. The "local" (in energy and search

region) significance of this excess has been estimated as 4.6 standard deviations [70]. However, FERMI/LAT themselves, using a slightly larger data sample and an improved algorithm to reconstruct the photons, later estimated the local significance to only 3.3 standard deviations [71]. Since the spectrum contains many independent bins, the global significance is estimated to 1.6 standard deviations in [71]. Ref. [70] cites a global significance of 3.2 standard deviations. This triggered a large amount of speculative work, but is well below the significance required of an unambiguous signal. Note that the cross section required to explain this feature through WIMP annihilation is larger than that predicted by nearly all models that have been suggested before ref. [70] was published.

All other observations by FERMI/LAT as well as by Cherenkov telescopes are in agreement with predictions based on purely astrophysical sources. In particular, a combination [72] of FERMI/LAT limits from dwarf galaxies excludes WIMPs annihilating hadronically with the standard cross section needed for thermal relics, if the WIMP mass is below 25 GeV; the main assumption is annihilation from an $S-$wave initial state. Carefully modeling continuum $\gamma$ emission from a region near (but excluding) the galactic center leads to similar upper bounds on the WIMP annihilation cross section [73]. These limits exclude many models with enhanced WIMP annihilation cross sections that had been designed to explain the electron and/or positron excess observed by PAMELA, FERMI/LAT and AMS02.

Antiparticles arise as additional WIMP annihilation products in the halo. To date the best measurement of the antiproton flux comes from the PAMELA satellite [30], and covers kinetic energies between 60 MeV and 180 GeV [74]. The result is in good agreement with secondary production and propagation models. These data exclude WIMP models that attempt to explain the $e^{\pm}$ excesses via annihilation into $W^{\pm}$ or $Z^0$ boson pairs; however, largely due to systematic uncertainties they do not significantly constrain conventional WIMP models.

The best measurements of the positron (and electron) flux at energies of tens to hundreds GeV comes from AMS02 [76] and PAMELA [75], showing a rather marked rise of the positron fraction between 10 and 200 GeV; the AMS02 data are compatible with a flattening of the positron fraction at the highest energies. While the observed positron spectrum falls within the one order of magnitude span (largely due to differences in the propagation model used) of fluxes predicted by secondary production models [77], the increase of the positron fraction is difficult to reconcile with the rather hard electron spectrum measured by PAMELA [78], if all positrons were due to secondary interactions of cosmic ray particles. Measurements of the total electron+positron energy spectrum by ATIC [79], FERMI/LAT [80] and H.E.S.S. [81] between 100 and 1000 GeV also exceed the predicted purely secondary spectrum, but with very large dispersion of the magnitude of these excesses. These observations can in principle be explained through WIMP annihilation. However, this requires cross sections well above that indicated by Eq. (24.6) for a thermal WIMP. This tension can be resolved only in somewhat baroque WIMP models. Most of these models have by now been excluded by the stringent bounds from FERMI/LAT on the flux of high energy photons due to WIMP annihilation. This is true also for models trying to explain the leptonic excesses through the decay of WIMPs with lifetime of the order of $10^{26}$ s. In contrast, viable astrophysical explanations of

these excesses introducing new primary sources of electrons and positrons, e.g. pulsars, have been suggested [15]. On the other hand, the high quality of the AMS02 data on the positron fraction, which does not show any marked features, allows one to impose stringent bounds on WIMPs with mass below 300 GeV annihilating directly into leptons [82].

Last but not least, an antideuteron signal [1], as potentially observable by AMS02 or PAMELA, could constitute a signal for WIMP annihilation in the halo.

An interesting comparison of respective sensitivities to MSSM parameter space of future direct and various indirect searches has been performed with the DARKSUSY tool [83]. A web-based up-to-date collection of results from direct WIMP searches, theoretical predictions, and sensitivities of future experiments can be found in [59]. Also, the web page [84] allows to make predictions for WIMP signals in various experiments, within a variety of SUSY models and to extract limits from simply parametrised data. Integrated analysis of all data from direct and indirect WIMP detection, and also from LHC experiments should converge to a comprehensive approach, required to fully unravel the mysteries of dark matter.

**References:**


1. For details, recent reviews and many more references about particle dark matter, see G. Bertone, *Particle Dark Matter* (Cambridge University Press, 2010).
2. For a brief but delightful history of DM, see V. Trimble, in *Proceedings of the First International Symposium on Sources of Dark Matter in the Universe*, Bel Air, California, 1994, published by World Scientific, Singapore (ed. D.B. Cline). See also the recent review G. Bertone, D. Hooper, and J. Silk, Phys. Rep. **405**, 279 (2005).
3. See *Cosmological Parameters* in this *Review*.
4. B. Paczynski, Astrophys. J. **304**, 1 (1986);
   K. Griest, Astrophys. J. **366**, 412 (1991).
5. F. De Paolis *et al.*, Phys. Rev. Lett. **74**, 14 (1995).
6. R. Catena and P. Ullio, JCAP **1008**, 004 (2010).
7. M. Pato *et al.*, Phys. Rev. **D82**, 023531 (2010).
8. J. Bovy and S. Tremaine, Astrophys. J. **756**, 89 (2012).
9. K. Kohri, D.H. Lyth, and A. Melchiorri, JCAP **0804**, 038 (2008).
10. See *Axions and Other Very Light Bosons* in this *Review*.
11. A. Kusenko, Phys. Reports **481**, 1 (2009).
12. E.W. Kolb and M.E. Turner, *The Early Universe*, Addison-Wesley (1990).
13. For a general introduction to SUSY, see the section devoted in this *Review of Particle Physics*. For a review of SUSY Dark Matter, see G. Jungman, M. Kamionkowski, and K. Griest, Phys. Reports **267**, 195 (1996).
14. See *Searches for WIMPs and Other Particles* in this *Review*.
15. M. Cirelli, Pramana **79**, 1021 (2012);
    S. Profumo, Central Eur. J. Phys. **10**, 1 (2011).
16. T. Moroi and L. Randall, Nucl. Phys. **B570**, 455 (2000).
17. R. Allahverdi and M. Drees, Phys. Rev. Lett. **89**, 091302 (2002).
18. M. Fujii and T. Yanagida, Phys. Lett. **B542**, 80 (2002).

19. J. Hisano, K. Kohri, and M.M. Nojiri, Phys. Lett. **B505**, 169 (2001).
20. D.E. Kaplan, M.A. Luty, and K.M. Zurek, Phys. Rev. **D79**, 115016 (2009).
21. G. Belanger *et al.*, arXiv:1308.3735.
22. J. Kozaczuk and S. Profumo, arXiv:1308.5705.
23. MACHO Collab., C. Alcock *et al.*, Astrophys. J. **542**, 257 (2000);
EROS Collab., AA **469**, 387 (2007);
OGLE Collab., arXiv:1106.2925 [astro-ph.GA],(MNRAS, to appear).
24. S.J. Asztalos *et al.*, Phys. Rev. **D69**, 011101 (2004);
S.J. Asztalos *et al.*, Phys. Rev. Lett. **104**, 041301 (2010).
25. L.D. Duffy *et al.*, Phys. Rev. **D74**, 012006 (2006);
J. Hoskins *et al.*, Phys. Rev. **D84**, 121302 (R) (2011).
26. M.C. Smith *et al.*, Mon. Not. R. Astron. Soc. **379**, 755 (2007).
27. J. Ellis *et al.*, Phys. Rev. **D77**, 065026 (2008).
28. C.E. Aalseth *et al.*, Phys. Rev. Lett. **106**, 131301 (2011).
29. XENON100 Collab., E. Aprile *et al.*, Phys. Rev. Lett. **109**, 181301 (2012).
30. A very useful collection of web links to the homepages of Dark Matter related conferences, and of experiments searching for WIMP Dark Matter, is the "Dark Matter Portal" at http://lpsc.in2p3.fr/mayet/dm.php. See TAUP and IDM conference series sites : http://www.taup-conference.to.infn.it/ and http://kicp-workshops.uchicago.edu/IDM2012/overview.php.
31. C.E. Aalseth et al., Phys. Rev. **D88**, 012002 (2013).
32. TEXONO Collab., H.B. Li et al., Phys. Rev. Lett. **110**, 261301 (2013).
33. https://commons.lbl.gov/display/TAUP2013/TAUP2013+Home.
34. C. Kelso et al., Phys. Rev. **D85**, 043515 (2012).
35. C.E. Aalseth et al., Phys. Rev. Lett. **107**, 141301 (2011).
36. CDMS Collab., Z. Ahmed et al., arXiv:1203.1309.
37. DAMA Collab., R. Bernabei *et al.*, Eur. Phys. J. **C67**, 39 (2010).
38. M. Fairbairn and T. Schwetz, JCAP **0901**, 037 (2009).
39. DAMA Collab., R. Bernabei *et al.*, Eur. Phys. J. **C56**, 333 (2008).
40. C.J. Copi and L.M. Krauss, New Astron. Rev. **49**, 185 (2005).
41. S.C. Kim et al., Phys. Rev. Lett. **108**, 181301 (2012).
42. http://vietnam.in2p3.fr/2013/Inauguration.
43. CDMS Collab., Z. Ahmed *et al.*, Science **327**, 1619 (2010).
44. CDMS Collab., Z. Ahmed *et al.*, to appear in Phys. Rev. Lett., arXiv:1304.4279.
45. CDMS Collab., R. Agnese *et al.*, Phys. Rev. **D88**, 031104 (2013).
46. SuperCDMS Collab., R. Agnese *et al.*, arXiv:1309.3259.
47. EDELWEISS Collab., E. Armengaud *et al.*, Phys. Rev. **D86**, 051701 (2012).
48. CDMS Collab., Z. Ahmed *et al.*, Phys. Rev. Lett. **06**, 131302 (2011).
49. EDELWEISS and CDMS Collab., Z. Ahmed *et al.*, Phys. Rev. **84**, 011102 (2011).
50. CRESST Collab., G. Angloher *et al.*, Eur. Phys. J. **C72**, 197 (2012).
51. XENON100 Collab., E. Aprile *et al.*, Phys. Rev. Lett. **111**, 021301 (2013).
52. XENON10 Collab., J Angle *et al.*, Phys. Rev. Lett. **107**, 051301 (2011).
53. M.T. Frandsen *et al.*, JCAP 1307 (2013) 023.
54. ZEPLIN Collab., D.Yu. Akimov *et al.*, Phys. Lett. **B709**, 14-20 (2012).

55. LUX Collab., D.S. Akerib *et al.*. arXiv:1310.8214.
56. E. Behnke *et al.*, Phys. Rev. Lett. **106**, 021303 (2011).
57. S. Archambault *et al.*, Phys. Lett. **B682**, 185 (2009).
58. M. Felizardo *et al.*., Phys. Rev. Lett. **108**, 201302 (2012).
59. DMTOOLS site : http://dmtools.brown.edu:8080/.
60. J. Billard, L. Strigari, E. Figueroa-Feliciano, arXiv:1307.545.
61. C. Savage *et al.*., JCAP **0904**, 010, 2009.
62. R. Trotta *et al.*., JHEP **0812** 024, 2008.
63. O. Buchmueller *et al.*., Eur. Phys. J. C72, 2243(2012).
64. M. Cahill-Rowley *et al.*., arXiv:1305.6921v2.
65. SuperKamiokande Collab., T. Tanaka et al., Astrophys. J. **742**, 78 (2011).
66. IceCube Collab., R. Abbasi *et al.*, Phys. Rev. **D85**, 042002 (2012).
67. IceCube Collab., M.G. Aartsen et al., Phys. Rev. Lett. **110**, 131302 (2013).
68. H.E.S.S. Collab., F. Aharonian *et al.*, Astron. Astrophys. **503**, 817 (2009); H.E.S.S. Collab., F. Acero *et al.*, MNRAS **402**, 1877 (2010).
69. M. Su, T.R. Slatyer, and D.P. Finkbeiner, Astrophys. J. **724**, 1044 (2010).
70. C. Weniger, JCAP **1208**, 007 (2012).
71. Fermi-LAT Collab., M. Ackermann et al., arXiv:1305.5597.
72. Fermi-LAT Collab., M. Ackermann et al., Phys. Rev. Lett. **107**, 241302 (2011).
73. Fermi-LAT Collab., M. Ackermann *et al.*, Astrophys. J. **761**, 91 (2012).
74. PAMELA Collab, O. Adriani *et al.*, Phys. Rev. Lett. **105**, 121101 (2010).
75. PAMELA Collab., O. Adriani *et al.*, arXiv:1308.0133.
76. AMS02 Collab., M. Aguilar *et al.*, Phys. Rev. Lett. **110**, 141102 (2013).
77. T. Delahaye *et al.*, Astronomy and Astrophysics **501**, 821 (2009).
78. PAMELA Collab., O. Adriani *et al.*, Phys. Rev. Lett. **106**, 201101 (2011).
79. ATIC collab, J. Chang *et al.*, Nature (London) **456**, 362 (2008).
80. FERMI/LAT collab, A.A. Abdo *et al.*, Phys. Rev. Lett. **102**, 181101 (2009).
81. H.E.S.S. collab, F. Aharonian *et al.*, Astron. Astrophys. **508**, 561 (2009).
82. L. Bergstrom *et al.*, arXiv:1306.3983.
83. DARKSUSY site: http://www.physto.se/ edsjo/darksusy/.
84. ILIAS web page: http://pisrv0.pit.physik.uni-tuebingen.de/darkmatter/.